Avrami theory for transformations from non-uniform austenite grain structures

H. Matsuda and H. K. D. H. Bhadeshia

Classical overall transformation kinetics theory for grain boundary nucleated transformations relies on the assumption that the parent phase grain size is uniform. In the present work the theory is adapted to deal with the case where there is a distribution in the size of the parent grains, as is often found in practice. It is demonstrated that the overall transformation rate is fastest when the starting grain structure is uniform. The method has been applied to the formation of allotriomorphic ferrite in austenite and the results have been compared against published experimental data. MST/5583

Introduction

It is never the case that an industrial material has a uniform grain size; when large steel beams are hot rolled into complex shapes, the plastic strain is not uniform and frequently leads to a bimodal distribution of austenite grains. On cooling, these grains transform into microstructures which are also non-uniform on a scale which leads to corresponding variations in mechanical properties.

The purpose of the work described here was to formulate an overall transformation kinetics model which describes grain boundary nucleated transformations in circumstances where the parent phase grains are not uniform in size. As is well known, the classical theory for randomly nucleated transformations is due to Johnson, Mehl, Avrami and Kolmogorov;[1–4] the version for grain boundary nucleated transformations from a uniform parent microstructure was developed later by Cahn.[5] It is these theories which form the basis of the present work; since the original ideas are well documented, they are not introduced in detail except when it is necessary to do so for the sake of clarity.

Method

The system of parent phase grains is classified into i categories such that

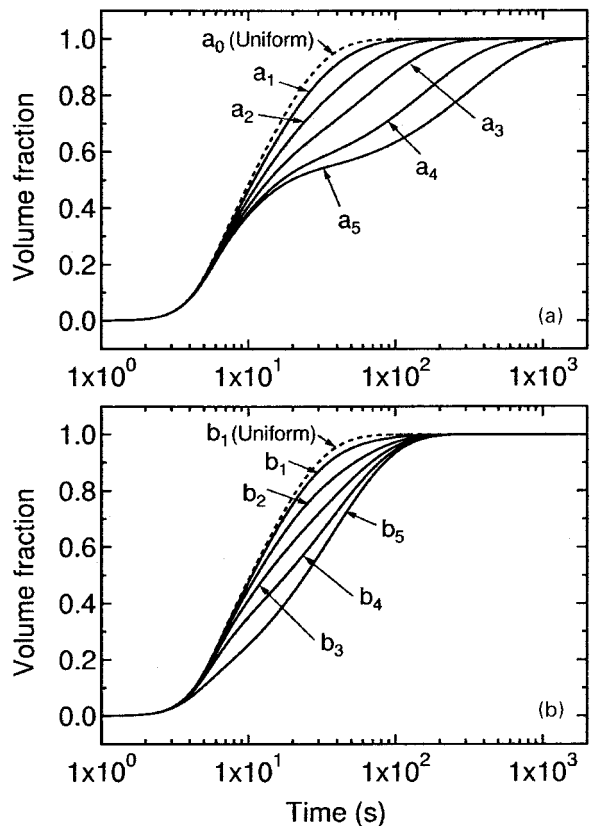$$V_T = \sum_i V_i \quad \text{and} \quad V_T S_V = \sum_i V_i S_{V_i} \quad \ldots \ldots \quad (1)$$

where V_T is the total sample volume and V_i is the volume of grains in category i. Similarly, S_V and S_{V_i} represent the total grain surface per unit volume and that due to category i, respectively.

If it is assumed that each category of parent γ grains transforms independently, then following Cahn[5]

$$V_{\alpha i} = V_i[1 - \exp\{-S_{V_i} f(I_B, G, t)\}] \quad \ldots \ldots \quad (2)$$

where $V_{\alpha i}$ is the volume of the product phase α in category i, I_B is the nucleation rate per unit area of grain boundary, G is the isotropic growth rate of α and t is the time at the isothermal transformation temperature. The function f has been derived by Cahn to be

$$f(I_B, G, t) = 2G^2 t \int_0^1 \left[1 - \exp \left\{ -\frac{\pi}{3} I_B G^3 t^3 \right. \right.$$
$$\left. \left. \times (1 - 3\xi^2 + 2\xi^3) \right\} \right] d\xi \quad \ldots \ldots \quad (3)$$
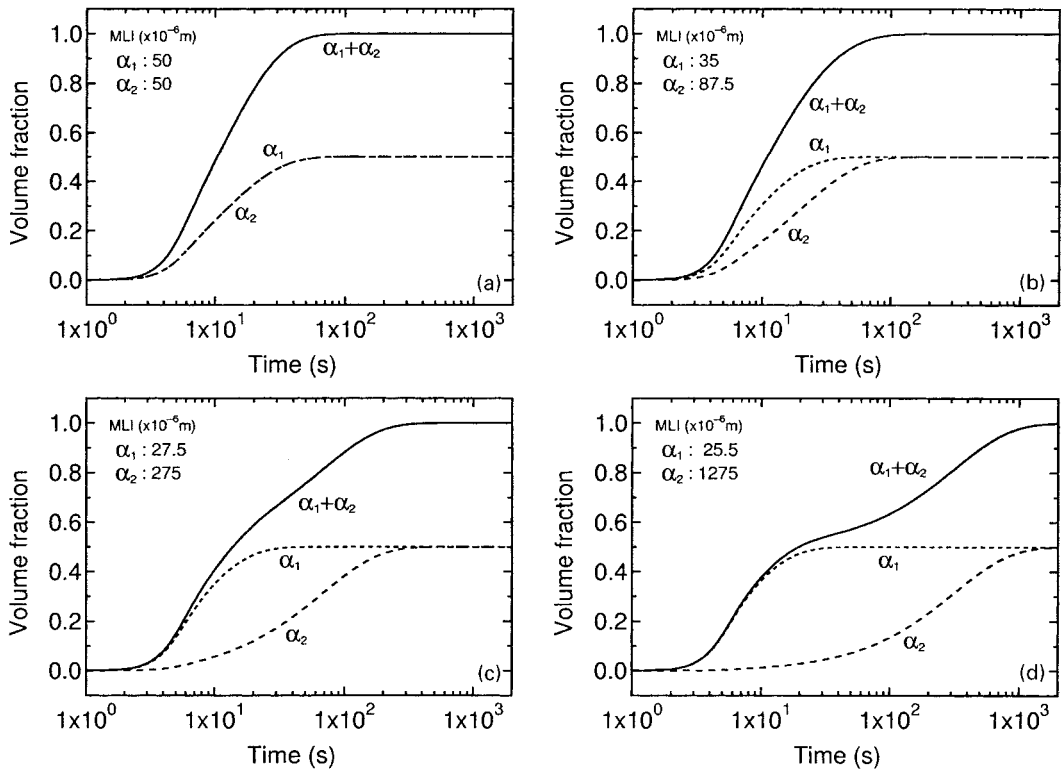

a mean linear intercept of each category of grain size is varied, while the volume fraction of each category is fixed at 0·5; *b* mean linear intercept of one category is set as 150 μm while the other parameters are varied

1 Calculated evolution of precipitate volume fraction with non-uniform parent grain structure: all parent grains are assumed to fall into two categories; the conditions for the calculations are listed in Table 1; average mean linear intercept is 50 μm in all cases

The total volume of α is then simply $V_\alpha = \Sigma_i V_{\alpha i}$ and its volume fraction $\Psi_\alpha = V_\alpha / V_T$.

Figure 1 shows the evolution of volume fraction of a new phase under several conditions; parameters of each category for the calculation are listed in Table 1. The average mean

a condition a_0; *b* condition a_1; *c* condition a_3; *d* condition a_5

2 Calculated evolution of volume fraction for each grain size category using parameters listed in Table 1: mean linear intercept of each category is varied, while the average mean linear intercept and the volume fraction of each category are fixed to 50 μm and 0·5, respectively

linear intercept of whole system is set as 50 μm in all conditions. The mean linear intercept of each category is varied while the volume fraction of each category is fixed to 0·5 in Fig. 1*a*. On the other hand, the mean linear intercept of one category is fixed to 150 μm while the other parameters are varied in Fig. 1*b*. The constant nucleation and growth rates are set as $1·0 \times 10^{10}$ m^{-3} s^{-1} and $1·0 \times 10^{-6}$ m s$^{-1/2}$, respectively. Figure 2 shows the evolution of precipitate volume fraction of each category under several conditions shown in Fig. 1*a*; the volumes of the two categories are identical in these conditions. Figure 3 shows the evolution of volume fraction of each category under several conditions shown in Fig. 1*b*. These results indicate that the transformation in the whole assembly is controlled by the large grains in the parent grain structure after the small parent grain structure has become saturated.

The results show consistently that the overall transformation rate is faster from a uniform γ grain structure when the latter is compared with a non-uniform structure with an identical S_V. This can be demonstrated mathematically by considering a two category γ grain structure in which the volume fraction of the first category is p and $S_{V_1} = kS_V$. To maintain the same total S_V in the uniform and non-uniform cases, it is necessary to impose the constraint

$$S_V = pS_{V_1} + (1-p)S_{V_2} \equiv pkS_V + (1-p)S_{V_2} \quad . \quad . \quad . \quad (4)$$

It follows from this that $p^{-1} > k > 0$ and

$$V_\alpha = pV_T[1 - \exp\{-kS_Vf\}] + (1-p)V_T$$
$$\times \left[1 - \exp\left\{ -\frac{1-pk}{1-p} S_Vf \right\} \right] \quad . \quad . \quad . \quad . \quad . \quad (5)$$

Table 1 Data set of mean linear intercept, grain boundary area per unit volume and volume fraction for the calculations shown in Fig. 1: the average mean linear intercept is 50 μm; for codes *a* mean linear intercept of each category is variable, but the volume fraction of each category is set as 0·5; for codes *b* mean linear intercept of one category is fixed at 150 μm and that of the other is varied; the volume of each category is adjusted to keeping the average mean linear intercept as 50 μm

Symbol	Mean linear intercept (μm)		Grain boundary area per unit volume ($\times 10^6$ m^{-1})		Volume fraction	
	Cat. 1	Cat. 2	Cat. 1	Cat. 2	Cat. 1	Cat. 2
a_0	50·0	50·0	0·0400	0·0400	0·5	0·5
a_1	35·0	87·5	0·0571	0·0229	0·5	0·5
a_2	30·0	150·0	0·0667	0·0133	0·5	0·5
a_3	27·5	275·0	0·0727	0·0059	0·5	0·5
a_4	26·0	650·0	0·0769	0·0031	0·5	0·5
a_5	25·5	1275·0	0·0784	0·0016	0·5	0·5
b_0	50	50	0·0400	0·0400	0·5000	0·5000
b_1	45	150	0·0444	0·0133	0·8780	0·1220
b_2	35	150	0·0571	0·0133	0·6512	0·3488
b_3	25	150	0·0800	0·0133	0·4444	0·5556
b_4	15	150	0·1333	0·0133	0·2553	0·7447
b_5	5	150	0·4000	0·0133	0·0816	0·9184
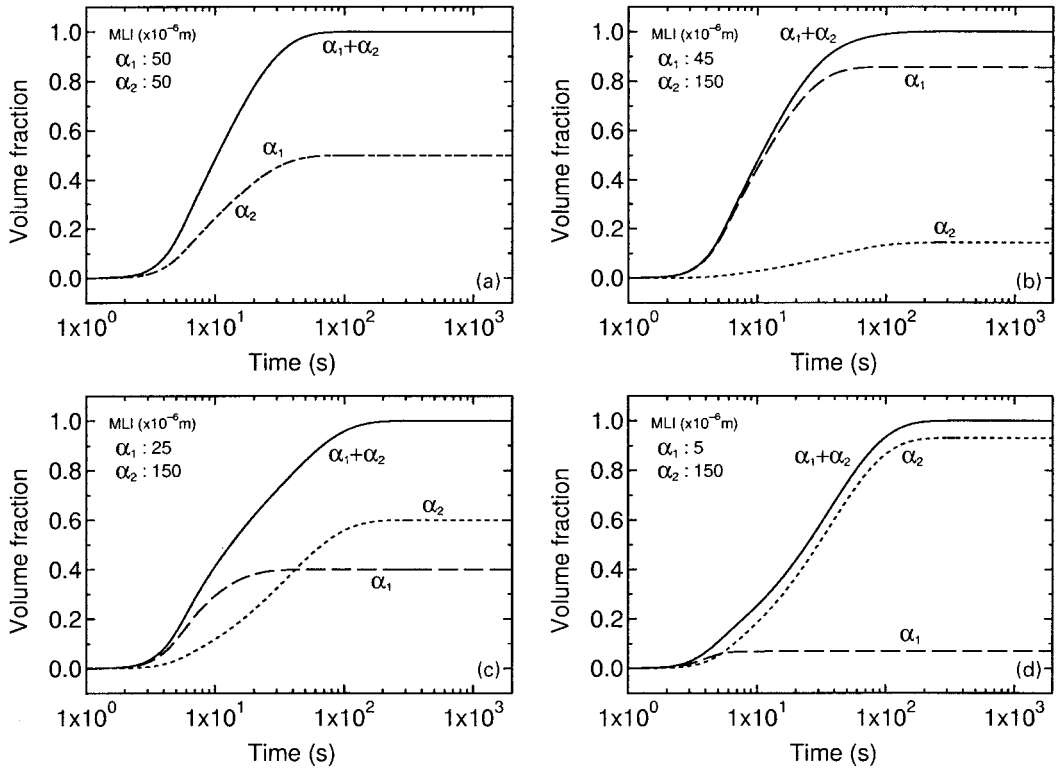
a condition b$_0$; *b* condition b$_1$; *c* condition b$_3$; *d* condition b$_5$

3   Calculated evolution of volume fraction for each grain size category using the parameters listed in Table 1: mean linear intercept of one category is fixed to 150 μm, while the other parameters are varied to keep the average mean linear intercept 50 μm

For a uniform grain structure

$$V_{\alpha,\text{uniform}} = V_T[1 - \exp\{-S_V f\}] \qquad \ldots \ldots \ldots \quad (6)$$

so

$$V_{\alpha,\text{uniform}} > V_\alpha$$

if

$$\frac{e^{-1}}{p \exp\{-k\} + (1+p) \exp\left\{-\frac{1-pk}{1-p}\right\}} < 1 \quad \ldots \ldots \quad (7)$$

which is the case for all values of p.

Allotriomorphic ferrite formation

The theory is now applied to the grain boundary nucleation and growth of allotriomorphic ferrite in steels; following previous studies,[6–11] the shape of a freely growing allotriomorph is assumed to be that of a disc parallel to the grain boundary. The nucleation rate is the sum of those as grain faces, edges and corners

$$I = I_f + I_e + I_c \qquad \ldots \ldots \ldots \ldots \ldots \ldots \quad (8)$$

where I_f, I_e, and I_c are the individual nucleation rate per unit area at the grain boundaries face, edge and corner respectively. The rate at each site is given by classical nucleation theory[12]

$$I_j = \frac{kT}{h} N_j \exp\left(-\frac{G_j^* + Q}{kT}\right) \qquad \ldots \ldots \ldots \quad (9)$$

where h is Planck's constant, k is Boltzmann's constant, T is the absolute temperature and Q is the activation free energy per atom for the transfer of atoms across the austenite/ferrite interface. N_j is the number of atomic sites per unit area that are available for nucleation and G_j^* is the critical

free energy of activation per atom; the subscript j denotes the type of grain site (face, edge and corner).

Assuming that each atom on the grain boundary may act as a potential site, the number of sites per unit area available for nucleation is

$$N_j = K_{1j} \frac{1}{2\delta^2} \qquad \ldots \ldots \ldots \ldots \ldots \ldots \quad (10)$$

where K_{1j} is a site factor which represents the fraction of sites that are active $\delta \approx 2 \cdot 5 \times 10^{-10}$ m is the interatomic spacing.[12] The relationship between the number densities of each type of site can be expressed as[5,11,12]

$$N_f = \frac{K_{1f}}{2\delta^2} \quad \text{and} \quad N_e = \frac{K_{1f}}{2\delta d_\gamma} \quad \text{and} \quad N_c = \frac{K_{1f}}{2d_\gamma^2} \qquad (11)$$

where d_γ is the mean linear intercept of γ. The activation energy for nucleation G_j^* is described as

$$G_j^* = K_{2j} \frac{\sigma_{\gamma\alpha}^3}{\Delta G_v^2} \qquad \ldots \ldots \ldots \ldots \ldots \ldots \quad (12)$$

where K_{2j} is the shape factor that takes into account the geometry of precipitate, $\sigma_{\gamma\alpha}$ is the interfacial energy per unit area between austenite and ferrite grains and ΔG_v is the free energy change per unit volume.

The interfacial energy $\sigma_{\gamma\alpha}$ per unit area between austenite and ferrite grains is taken as a constant $0 \cdot 05$ J m^{-2} (Refs. 11, 13–15). ΔG_v is calculated using a parallel tangent construction, as a function of temperature and alloy chemistry.[16] Q is taken as $4 \cdot 0 \times 10^{-19}$ J, which corresponds to 241 kJ mol^{-1} (Ref. 11). K_{1f}, K_{2f}, K_{2e} and K_{2c} are constants determined by fitting to experimental data,[17] taken to be $1 \cdot 5 \times 10^{-12}$, $2 \cdot 0 \times 10^{-1}$, $1 \cdot 0 \times 10^{-2}$ and $1 \cdot 0 \times 10^{-3}$, respectively.

Allotriomorphs are able to grow on both sides of the austenite grain boundary. The growth is assumed to be diffusion-controlled under paraequilibrium condition. The
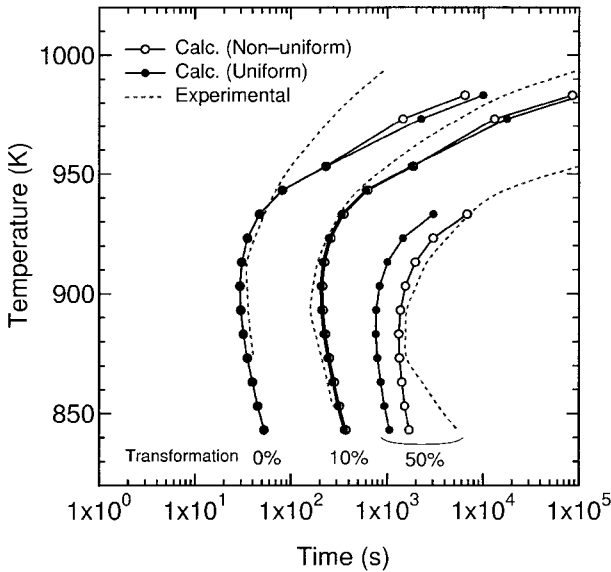
4 **Calculated and experimental C curves in TTT diagram for steel shown in Table 2: experimental curves are from previous research;[17] the parameters of each condition for calculation are listed in Table 3**

half-thickness q normal to grain boundary and the radius r_w of each allotriomorph parallel to grain boundary during isothermal transformation is given by

$$q = \lambda(t-\tau)^{1/2} \quad \text{and} \quad r_w = \kappa\lambda(t-\tau)^{1/2} \quad . \quad . \quad . \quad . \quad (13)$$

respectively, where λ is the one-dimensional parabolic thickening rate constant and $\kappa = 3$ is the aspect ratio.[18,19]

The calculation of the rate constant λ is completed using a concentration dependent diffusion coefficient of carbon in austenite. It was calculated numerically according to a published procedure.[20,21] The diffusivity of carbon was calculated as a function of temperature and chemical composition as in Refs. 22 and 23.

Numerical method

Cahn's overall transformation kinetics theory for grain boundary nucleated reactions has been implemented into a flexible numerical scheme by Jones and Bhadeshia.[8–10] Since the details of the method have been described in detail in the original publications, they are not reproduced here except to point out the numerical approach is necessary in order to take account of changing boundary conditions due to soft impingement and continuous cooling transformation.

Figure 4 shows both the calculated and experimental C curves of a TTT diagram[17] for the steel in Table 2. Calculations are performed assuming both uniform and non-uniform grain structures; the parameters for each grain structure are shown in Table 3. The curves for transformation start and 10% transformation shows almost no

difference between the results of uniform structure and that of non-uniform structure; these both agree with the experimental results except at high temperature (950 K). On the other hand, there is a difference between uniform and non-uniform structures for calculating the 50% transformation time. The result for the non-uniform grain structure is more consistent with the experimental result than that for the uniform structure. Figure 5 shows the calculated evolution of volume fraction of allotriomorphic ferrite for uniform and non-uniform grain structures. These figures demonstrate that the difference between the result of the uniform structure and that of the non-uniform structure is caused by suppression of the transformation by the larger grain size in the non-uniform structure as discussed before.

Although only the ASTM number is given and there is no further information available about the grain size distribution that gave the experimental result,[17] it is believed that the sample for the experiment probably had grain size distribution. Therefore, the calculation for non-uniform grain structure is more accurate. This effect of grain size distribution may be one of the reasons for discrepancies in the experimental and calculated results. Thus it is a possible to get more accurate results when the grain boundary size distribution is taken into account. The calculations have bigger discrepancies at temperatures above 940 K for the 0 and 10% curves, and at temperatures below 870 K for 50% transformation. The discrepancy at high temperatures is because the calculation was done under the assumption of paraequilibrium condition in which the substitutional alloying elements do not partition during transformation. The discrepancy at low temperatures is because of carbide precipitation which consequently reduces carbon content in residual austenite.

Summary

Classical overall transformation kinetics theory for grain boundary nucleated transformations has been adapted in this work to deal with the case where the parent phase grains exhibit a nonuniform grain structure. An implicit assumption in the adaptation is that the heterogeneous grain structure can be treated as a series of independent categories of uniform grain structures. It is found that the transformation rate is fastest when the starting grain is uniform, in circumstances where the two microstructures are compared at a constant grain surface per unit volume. The method has been applied to the formation of allotriomorphic ferrite in austenite and the results are found to compare favourably against published experimental data.

Table 2 **Chemical compositions and ASTM grain size number of the steel (sample En16 in Ref. 17)**

Chemical composition, wt-%						ASTM grain size no.
C	S	Mn	Cr	Mo	Ni	
0·33	0·18	1·48	0·16	0·27	0·26	8·0

Table 3 **Data set of mean linear intercept, grain boundary area per unit volume and volume fraction used in calculations**

Symbol	Mean linear intercept(μm)		Grain boundary area per unit volume($\times 10^6$ m^{-1})		Volume fraction	
	Cat. 1	Cat. 2	Cat. 1	Cat. 2	Cat. 1	Cat. 2
Non-uniform	60	5	0·0333	0·4000	0·8182	0·1818
Uniform	20	20	0·1000	0·1000	0·5000	0·5000
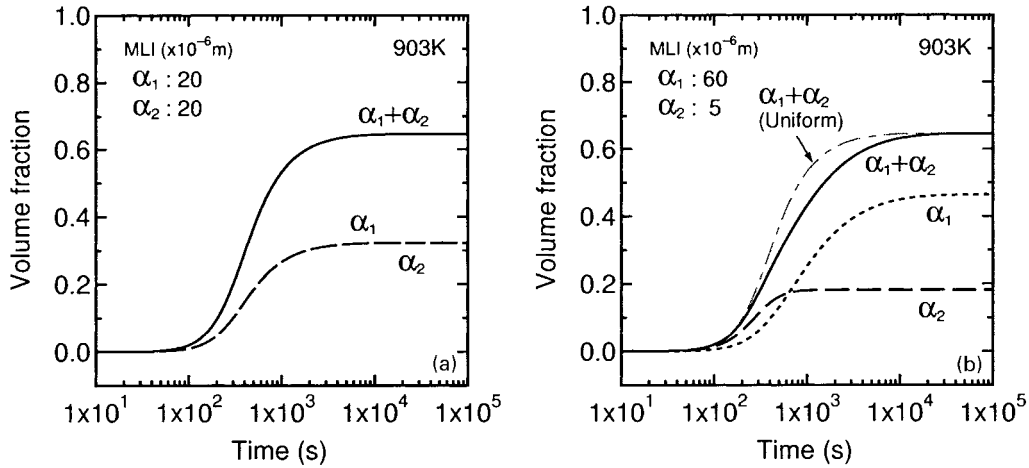
5 Calculated evolution of volume fraction of allotriomorphic ferrite: all grains are assumed to fall into two categories; mean linear intercept in the whole system is set as 50 μm in both conditions

References

1. M. AVRAMI: *J. Chem. Phys.*, 1939, **7**, 1103–1112.
2. W. A. JOHNSON and R. F. MEHL: *Trans. AIME*, 1939, **135**, 416–458.
3. M. AVRAMI: *J. Chem. Phys.*, 1940, **8**, 212–224.
4. M. AVRAMI: *J. Chem. Phys.*, 1941, **9**, 177–184.
5. J. W. CAHN: *Acta Metall.*, 1956, **4**, 449–459.
6. H. K. D. H. BHADESHIA, L-E. SVENSSON and B. GRETOFT: in 'Welding metallurgy of structural steels', (ed. J. Y. Koo), 517–529; 1987, Warrendale, PA, TMS.
7. R. C. REED and H. K. D. H. BHADESHIA: *Mater. Sci. Technol.*, 1992, **8**, 421–435.
8. S. J. JONES and H. K. D. H. BHADESHIA: *Acta Mater.*, 1997, **45**, 2911–2920.
9. S. J. JONES and H. K. D. H. BHADESHIA: *Metall. Trans. A*, 1997, **28A**, 2005–2013.
10. S. J. JONES: 'Modelling inclusion potency and simultaneous transformation kinetics in steels', PhD thesis, University of Cambridge, UK, 1996.
11. S. V. PARKER: 'Modelling of phase transformations in hot-rolled steels', PhD thesis, University of Cambridge, UK, 1996.
12. J. W. CHRISTIAN: 'The theory of transformation in metals and alloys', 2nd edn., Part 1: 'Equilibrium and general kinetic theory'; 1975, Oxford, Pergamon.
13. W. F. LANGE III, M. ENOMOTO and H. I. AARONSON: *Metall. Trans. A*, 1988, **19A**, 427–440.
14. W. F. LANGE III, M. ENOMOTO and H. I. AARONSON: *Int. Mater. Rev.*, 1989, **34**, 125–150.
15. M. ENOMOTO, W. F. LANGE III and H. I. AARONSON: *Metall. Trans. A*, 1986, **17A**, 1399–1407.
16. H. K. D. H. BHADESHIA: *Metal Sci.*, 1982, **16**, 159–165.
17. 'Atlas of isothermal transformation diagrams of BS En steels', 2nd edn; 1956, London, The Iron and Steel Institute.
18. J. R. BRADLEY and H. I. AARONSON: *Metall. Trans. A*, 1977, **8A**, 317–322.
19. J. R. BRADLEY, J. M. RIGSBEE and H. I. AARONSON: *Metall. Trans. A*, 1977, **8A**, 323–333.
20. C. ATKINSON: *Acta Metall.*, 1967, **15**, 1207–1211.
21. C. ATKINSON: *Acta Metall.*, 1968, **16**, 1019–1022.
22. H. K. D. H. BHADESHIA: *Met. Sci.*, 1981, **15**, 477–479.
23. S. S. BABU and H. K. D. H. BHADESHIA: *J. Mater. Sci. Lett.*, 1995, **14**, 314–316.